PLANE-STRAIN EXPERIMENT ON SOFT SEDIMENTARY ROCK

Guanlin Ye[1], Feng Zhang[2], Atsushi Yashima[3], Hla Aung[4] and Kiyokaza Naito[5]

ABSTRACT

It is recognized that the intermediate principal stress plays an important role on the strength and stress-dilatancy relation of soft sedimentary rock. However few plane-strain/true triaxial experiments on soft rock can be seen due to the difficulties of experiment with relatively high-strength geomaterial. The traditional plane-strain apparatus, which was equipped with a pre-fixed type plane-strain confining frame, is difficult to obtain a real isotropic consolidation before shearing. And the influence of membrane to high-strength specimen is seldom studied. On the other hand, although a lot of theoretical researches on clay/sand under general stress state have been done, such as Lade mode and tij model, their application to soft rock is not confirmed yet. This paper presents a combination of experimental and theoretical approaches for a better understanding of mechanical behaviors of soft rock. Firstly, a newly designed plane-strain test system for soft rock that has overcome the shortcomings of traditional type was introduced. And then some interesting results of the drained compression tests and drained creep tests along with theoretical simulations were given out. Finally the influences of

1 Researcher, Geo-Research Institute, 4-3-2, Itachibori, Nishi-ku, Osaka, 550-0012
2 Professor, Department of Civil Engineering, Nagoya Institute of Technology, Showa-ku, Gokiso-cho, Nagoya, 466-8555
3 Professor, Department of Civil Engineering, Gifu University, Yanagido 1-1, Gifu 501-1193
4 Researcher, Tokyo office of Geo-Research Institute, 1-8-4 Yushima, Bunkyo-ku, Tokyo 113-0034
5 Former graduate Student, Department of Civil Engineering, Gifu University, Yanagido 1-1, Gifu 501-1193

the membrane and filter paper were explained by a simple FEM.

Keywords: plane-strain experiment, soft sedimentary rock, drained shear, drained creep, membrane, FEM

INTRODUCTION

It is well known that the mechanical behavior of soft sedimentary rock is largely dependent on stress condition. The influence of the intermediate principal stress may greatly affect the strength and stress-dilatancy relation of geologic materials under different loading paths. During last few decades, a lot of plane-strain/true triaxial experiments have been done on clay and sand. Yet few plane-strain/true triaxial experiments on soft rock can be seen due to the difficulties of experiment with relatively high-strength geomaterial.

Some experimental researches have been carried out in recent years. Nishigami et al. (1993) employed artificial soft rock in their plane-strain tests and demonstrated the influence of intermediate principal stress. Hayono et al.(1999) developed a plane-strain and a true triaxial testing system that utilized the LDT (Local Deformation Transducer) to measure the local strain, and carried out a series of experiments on soft rock to evaluate its deformation characteristics at very small strain level. However, many geotechnical problems concerning with soft sedimentary rock, such as the progressive failure of soft rock slope (e.g., Yashima et

al., 1999) and the construction of tunnel in strong weathered soft rock ground, are linked to the stress-strain relation from the start of shearing to totally failure.

In traditional plane-strain apparatus, the specimen encapsulated with rubber membrane was firstly installed into the conventional fixed type of confining platens with a certain preload, and then placed into the hydraulic pressure cell to achieve a so-called isotropic consolidation condition. However, it is difficult to keep the consolidation be isotropic because the specimen will contract during the consolidation, and the influence (bedding error) of the membrane is unknown. Furthermore, as the cap was fixedly connected with the axial loading rod which is locked during consolidation, a recessing deformation will occur when the specimen contracts, as showing in Fig. 1, especially when the specimen is relatively compressible. This is to say, a uniform deformation/stress of the specimen also cannot be guaranteed.

On the other hand, a lot of theoretical researches on the strength and deformation properties of sand/clay under general stress state have been done, such as Lade model (Lade, 1977) and tij clay/sand model (Nakai and Matsuoka 1986, Nakai 1989). The tij-concept can be described uniquely the stress-dilatancy relations of clay and sand. But the application to soft rock is leaved to be confirmed. An elasto-viscoplastic constitutive model for soft rock using tij concept and subloading surface (Hashiguchi, 1977) was proposed by Zhang et al. (2005). This model can not only describe the time-dependency behavior of soft rock but also take into consideration the influence of intermediate principal stress.

Therefore, in order to investigate the stress-dilatancy relation at relatively large strain level of soft sedimentary rock under general loading condition, we developed a new plane-strain apparatus with countermeasures for aforementioned potential hardware-related problems, and carried out a systematical series of plane-strain/triaxial compression and creep tests. In present paper, the apparatus is described firstly with focus on some improvement points. Specimen preparation and test procedure are then explained. Secondly, some experiment results and their analysis (using tij-concept) are given out. Lastly, element simulations by Zhang's model are carried out, and discrepancies between theoretical value and the observed data are found. The reason of the discrepancies, namely, the influence of membrane and filter paper, is investigated carefully by a simple FEM and experiments.

TEST APPARATUS

Fig. 2 shows the photo of the plane-strain test system. It consists of a hydraulic pressure cell, independent axial and transverse loading units, a control system for air pressure and axial loading with stress and strain controlling, and a data acquisition system. Fig. 3 shows the schematic illustration of the hydraulic pressure cell.

It is known that uniaxial compression strength of soft rock is usually up to about 20MPa. Underground structures constructed in soft rock ground, such as the storages for high-level waste disposal and compressed air energy, are usually constructed several hundred meters

beneath ground surface, where the confining stress is as high as several MPa. Therefore, a maximum capacity of an axial force up to 100kN and a cell pressure of 5MPa were designed to provide a suitable range of loading condition necessary for the soft rock concerned.

Post-Confining platen

As mentioned in the INTRODUCTION, the traditional plane-strain apparatus is difficult to achieve a real isotropic consolidation condition before shearing. In order to satisfy this consolidation and in the same time provide a plane-strain condition during shearing, a new kind of plane-strain platens were designed, in which two constraint steel platens linked by four rods form a plane-strain frame, as shown in Fig. 4. One side of the rods is fixed in one platen, and the other side can be clamped by oil-driven clutch embedding in the opposing platen. Each clutch is supplied by an oil pressure of 70MPa by which the total champing force may reach to 100kN. After the consolidation is finished, two platens can then be pushed from outside of the hydraulic pressure cell to contact the specimen, and the rods are fixed by the clutches and form a rigid plane-strain frame.

Separable Interface between axial load rod and cap

In order to avoid the recessing deformation that showed in Fig.1. A separable interface was adopted instead of conventional inseparable type. As show in Fig.5, two platens consisting of

two complementary spherical surfaces with different radiuses are set up in the connection part of axial load rod and cap. These two spherical surfaces form a gap, which make it possible to apply a cell water pressure to the cap during isotropic consolidation, while the axial load rob is locked. During shearing, however, two platens touch each other and work as a common load transferring device.

The authors would like to emphasize that both the post-confining platen and separable interface are indispensable for achieving a real isotropic consolidation condition.

Measurement

In creep test, strain develops very slowly during transient creep while quickly during accelerating creep. In order to obtain an accurate measurement of the strain in a reasonable time interval, high precision sensor is necessary. Two gap sensors as shown in Fig. 3 with a precision of 0.001mm, were set inside of the hydraulic pressure cell so as to measure accurately the axial displacement. A comparison with normally used displacement transducer (DT), shown in Fig. 3, whose precision is 0.01mm and was set outside of hydraulic pressure cell, is shown in Fig. 6. It indicates that a high precision tool is definitely needed to obtain a smooth and continuous changing curve of displacement during creep tests. Moreover, in order to measure accurately the lateral displacements of specimen, two more gap sensors were set transversely inside of the hydraulic pressure cell to measure the lateral displacement.

Inner porewater pressure

As to the reasons of strain-softening and creep behaviors of geomaterials, some researchers insisted that they are merely a result of boundary condition (eg. soil-water interaction, initial imperfection), and some other researchers persisted that they are the inherent properties of geomaterials. Although some conventional triaxial drained tests have been carried out to verify above theories and their results can be found on many literatures, however, in those tests, the loading path was limited to axial-symmetric condition and the pore water pressure near or inside shear band of the specimens were not clarified yet. Therefore, in order to verify the change of pore water pressure near or within a shear band formed in post-peak shearing process, a piezometer was set at the center of the specimen in addition to the one set at the bottom, as shown in Fig. 7. It is found in the tests that if the shear strain rate is slower than 0.001%/min, the influence of inner EPWP can be neglected, therefore ‘drained test’ is valid. The detail description of the test results and some finite element analyses on the inner pore water pressure can be referred to Zhang et al. (2006).

SOFT ROCK SPECIMEN PREPARATION

The soft sedimentary rock specimens used in this study were Ohya Stones, which were mined by block sampling at a depth from 30～60m in Tochigi Prefecture, Japan. The size of

plane-strain specimen is 200mm in height, 100mm in width and 80mm in thickness, while the size of specimen in triaxial test is 50mm in diameter and 100mm in height, as shown in Fig. 8.

Due to the relatively large size of the specimen and the limitation of current vacuum pump, to achieve a satisfied saturated state by vacuuming is impossible. It is found that B value, which represents the degree of saturation, only could acquire a value of 0.9 by vacuuming. Therefore, CO_2 gas was used before vacuuming to replace the air in the specimen. The saturation procedure is shown in Fig. 9. Since the CO_2 gas is much easier to melt into the water than air, the B value can be increased to a value larger than 0.95, which mean the specimen was almost fully saturated.

Because the mechanical behavior of soft rock will change a lot if the samples are open to air for a long time, experiments have to be done immediately after sampling. Meanwhile, before all the tests are finished, all the specimens are saturated and stocked in desiccate, as shown in Fig. 9(c).

Furthermore, following treatments were made to eliminate the boundary errors.

Firstly, in order to reduce the initial imperfection, the rock samples were fabricated accurately to prismatic specimens with a maximum uneven of 5um for all six faces.

Secondly, in order to reduce the friction at the faces of the specimen, two pieces of PTFE sheets coated with silicon grease were placed at every contacted face of specimen/membrane and devices, namely, in the cap and pedestal and the constraint platens as shown in Fig. 4.

With this treatment, the friction between the sample and the restriction platen can be effectively eliminated.

Thirdly, in order to shorten the test time in drained consolidation, drained paths made of striped filtering papers were covered on the specimen as shown in Fig. 8(b).

TEST PROCEDURE

After being isotropically consolidated for 24 hours under prescribed confining pressure, the specimen was subjected to drained constant-strain-rate compression test or drained creep test. In the drained compression test, the axial strain rates were controlled at 0.001%/min, which insured the influence of inner EPWP can be neglected. In creep test, instead of being applied abruptly, the axial load was applied with a prescribed constant axial force rate till the specified creep stress was reached. The patterns of the compression and creep tests are listed in Table 1 &2.

RESULTS OF TEST AND SUMMARIES

This session includes two parts, first is the investigation of drained constant strain rate tests. Base on the test results, tij-concept based stress-dilatancy relation and Cam-clay type stress-dilatancy relation are investigated and discussed in detail.

The second part will be focused on the drained creep tests, which are different from most of

previous undrained experiments.

Drained constant-strain-rate compression tests

A comparison of peak values of different types of stress ratio for the soft rock under plane-strain compression and conventional triaxial compression tests was conducted. The conventional triaxial compression tests (Takigawa, 2003) were conducted with different test apparatus but the test samples are the same as those used in the plane-strain compression tests. In the discussion, $\sqrt{2J_2}/\sigma_m^{'}$, where J_2 is the second invariant of deviatoric stress tensor and $\sigma_m^{'}$ is the mean effective stress, is a typical stress ratio used in Cam-clay type constitutive model, while t_S/t_N is a stress ratio based on tij-concept (Nakai & Matsuoka, 1986) and its brief description can be found in Appendix. Fig. 10(a) shows that there is no significant difference between the peak values of stress ratio $\sqrt{2J_2}/\sigma_m^{'}$ from two different tests. On the other hand, the peak values of stress ratio t_S/t_N, as shown in Fig. 10(b), are totally different under two different confining conditions, which indicates that the tij-concept can give a more proper description of the influence of intermediate principal stress of soft rock on strength under different stress conditions than Cam-clay type failure criterion can do.

Fig. 11 shows a comparison of volumetric strain under the plane-strain compression and triaxial compression. In both tests, the specimen contracted at first and then turned to expand. The quantity of expansion decreased as confining stress increased. And the volumetric

expansion under plane-strain compression was much smaller than that under triaxial compression because the plane-strain frame kept the specimen from expansion.

The stress-dilatancy relations obtained from aforementioned two compression tests in terms of stress ratio $\sqrt{2J_2}/\sigma_m^{'}$ vs. strain ratio $d\varepsilon_v / d\sqrt{e_{ij}e_{ij}}$ and stress ratio t_S / t_N vs. strain ratio $d\varepsilon_{SMP}^{*} / d\gamma_{SMP}^{*}$, are also investigated carefully. Here, ε_v is volumetric strain and e_{ij} is deviatoric strain tensor. A brief description of $d\varepsilon_{SMP}^{*} / d\gamma_{SMP}^{*}$ can be seen in Appendix. From Fig. 12, it can be seen that stress-dilatancy relations under varies of stress conditions depicted in terms of $\sqrt{2J_2}/\sigma_m^{'}$ and $d\varepsilon_v / d\sqrt{e_{ij}e_{ij}}$ scatters in a wide range while those depicted based on the tij-concept shows a intimate correlation, which make it easier to establish a proper plastic potential for a constitutive model of soft rock. In other words, the stress-dilatancy relation in terms of t_S / t_N vs. $d\varepsilon_{SMP}^{*} / d\gamma_{SMP}^{*}$ should be adopted in the constitutive model for soft rock other than $\sqrt{2J_2}/\sigma_m^{'}$ vs. $d\varepsilon_v / d\sqrt{e_{ij}e_{ij}}$.

Drained creep tests

The results of drained creep tests under plane-strain condition were investigated. Three drained creep tests under confining stress of 1.0 MPa were carried out, as listed in Table 2.

Fig. 13 shows the relations of axial strain rate vs. time and volumetric strain rate vs. time in logarithmic coordinate. The general characteristics of creep behavior such as initial creep rate, steady creep stage and creep rupture were clearly observed. The 95% and 90% creep tests

exhibited a typical creep rupture after being loaded for 1 day, while 85% did not fail even after being loaded for ten days. It can be seen clearly from the figure that the creep rupture time depends on creep stresses applied to the specimens. The larger the creep stress is, the faster the creep failure will occurs.

Fig. 14 shows the volumetric strain vs. time. The 95% and 90%, which showed creep rupture, exhibited a volume expansion. While the 85%, in which no failed was observed, exhibited a volume contraction.

ELEMENT SIMULATION OF PLANE-STRAIN COMPRESSION TEST

According to previous session, Zhang et al. (2005) developed an elasto-viscoplastic model for soft sedimentary rock. In this model, a plastic potential function in terms of tij-concept was adopted so as to describe not only time dependency such as strain rate dependency and creep but also strain hardening-strain softening behavior of soft rock under general stress conditions. Detailed descriptions of the model can be found in the work by Zhang et al. (2005). The drained triaxial and plane-strain compression and creep tests of Ohya Stones were simulated by this model.

The physical properties and the material parameters are listed in Table 3&4 respectively. Axial strain rate in simulation is identical to that in actual tests, 0.001%/min.

Fig. 15 represents the comparison between the theoretical and experimental stress-strain

relations and stress-dilatancy relations under triaxial loading. It was found from the figures that the model can predict the mechanical behavior of soft rocks with acceptable accuracy. Fig. 16 shows the comparison of plane-strain tests. Axial stress σ_1 and confining stress σ_2 as well as volumetric strain ε_v are plotted to represent the stress-strain-dilatancy relation. On the whole, the simulations are fit with the observed ones, especially with respect to σ_1 and ε_v. That is to say, the model can successfully describe the strain-softening and dilatancy properties of soft rock and take into consideration the influence of intermediate principal stress.

However, it is also found that the simulation values of σ_2 are much larger than the observed ones. The same finding also reported by Aung et al. (2004). The conceivable reasons might be that the specimen did not undergo a true plane-strain condition during the tests. In the test, the specimen was pasted with 2 pieces of stripped filter papers and then covered by a piece of membrane, and finally setup between two pieces of plane-strain confining platen. The filter paper and membrane is assigned as ‘covering material’ in this paper. Although the plane-strain confining platens are stiff enough to provide a plane-strain condition for the things inside, potential deformation of the covering materials, which are compressible, will make it fail to maintain a plane-strain condition for the specimen. Consequently it will bring about an underestimation of intermediate principal stress. Therefore, a finite element analysis was employed to investigate the reason.

AN INVESTIGATION INTO THE INFLUENCE OF COVERING MATERIALS BY FEM

Fig. 17 shows the FEM model for this investigation. Due to the symmetry, only 1/4 specimen is analyzed. This FEM model is so simple that can be executed by anyone with basic FEM knowledge. The material parameters for soft rock are the same as those in Table 4. The material properties of membrane and filter paper were not clear now so that the parameters listed in Table 5 were arbitrarily chosen, but also considered to be in a reasonable range.

The analyses with only soft rock (Elem 1) and membrane (Elem 3) were shown in Fig. 18. From Fig. 18 it can be seen the peak values of σ_2 obtained from FEM are much smaller than those in element simulation, and show no strain-softening behavior, but the residual values are the same as those of element simulation.

Furthermore, the influence of filter paper (Elem 2) was taken into consideration. Fig. 19 shows a comparison of calculations with/without filter paper, it can be seen that due to the additional compression of filter paper, not only the peak but also the residual strengths drop down a little, and the volumetric expansions become a little smaller. In summary, the amount of lateral expansion of specimen is not only depending on the compressibility of covering material, but also depending on thickness of the covering material.

At last, FEM calculations with membrane and filter paper are compared with the test, as shown in Fig. 20. Although the values of σ_2 are still larger then observed ones, their changing tendencies become close to the observed ones.

Experimental verification of membrane influence on plane-strain specimen

Two kinds of plane-strain compression test with rubber-block specimen (linear elastic material) with/without membrane, which covered the faces of intermediate principal stress directions as shown in Fig. 21 were conducted. The tests were performed under confining pressure of 1.0MPa with a shearing strain rate of 0.001 %/min. The difference is that one specimen was directly applied for loading while the other specimen was undergone the isotropic compression for 24 hours firstly. The photos of rubber plane-strain specimen with/without membrane are shown in Fig. 21. The observed stress-strain relations of the tests are shown in Fig. 22. The results show that the observed amount of intermediate principal stress depends on the existence of membrane covering material as well as isotropic compression applied to specimen before shearing, especially at the early stage of shearing.

Based on observed results, it is necessary to perform isotropic consolidation process before shearing to get enough fitting between membrane and specimen.

CONCLUSION

In present paper, a newly designed plane-strain test system for soft rock was introduced. And then some interesting results of the drained compression tests and drained creep tests were given out. Based on the experimental findings, a new elasto-viscoplastic model was proposed by Zhang et al. (2005). And the influences of the covering materials were explained by a simple FEM with this model. From this study, some conclusions can be obtained.

1) The newly designed test system, which can provide a real isotropic consolidation condition before shearing and an accurate measurement of strain, can produce a satisfactory test results for soft rock, including drained plane-strain tests and drained creep tests.

2) The tij-concept can give a more proper description of the influence of intermediate principal stress of soft rock on strength under general stress conditions than Cam-clay type failure criterion can do. And the stress-dilatancy relations based on tij-concept has an intimate correlation. Accordingly, a new elasto-viscoplastic model for soft rock was established by Zhang et al. (2005).

3) By using a finite element analysis, the influence of membrane and filter paper was investigated carefully. It is found that the compression of membrane will lead to a significant decrease of peak value of σ_2. If the compression of filter paper is considered, not only the peak but also the residual value of all mechanical quantity σ_1, σ_2 and ε_v will decrease. However the amount of decrease of σ_2 is more conspicuous than the others.

4) Nevertheless, the simple finite element analysis can help us to identify the mechanical

behavior of soft rock specimen under pseudo plane-strain conditions, and consequently the validity of a proposed constitutive model.

5) The combination of experimental and theoretical approaches is a useful tool for a better understanding of the mechanical properties of geomaterials.

REFERENCES

1) Aung H., Yashima A., Zhang F., Naito K. & Ye G.L. (2004): Strain softening with positive dilatancy and time dependency of soft sedimentary rock. Proc. of 2st International Workshop on New Frontiers in Computational Geotechnics (in printing).

2) Hashiguchi, K. (1980): Constitutive equation of elastoplastic materials with elasto-plastic transition, Jour. of Applied Mechanics, ASME, 102(2), 266-272.

3) Hayano K., Maeshiro T., Tatsuoka F., Sato T., Wang L. and Kodaka T. (1999): Shear banding in a sedimentary soft mudstone subjected to plane strain compression: ・ Geotechnical Testing Journal, No.1, Vol.22, pp.67-79

4) Lade, P.V. (1977): Elasto-pastic stress-strain theory for cohesionless soil with curved yield surfaces. International Journal of solids and structures, Vol.13, pp1019-1035.

5) Nakai T. and Matsuoka H. (1986): A generalized elastoplastic constitutive model for clay in a three-dimensional stresses, Soils and Foundations, Vol.26, No.3, pp 81-89.

6) Nakai. T. (1989): An isotropic hardening elastoplastic model for sand considering the stress path dependency in three-dimensional stresses, Soils and Foundations, Vol.29, No.1, pp 119-137.

7) Takigawa, M. (2003): Experimental study on the time dependent behavior of soft rock. Bachelor thesis of Gifu University.

8) Nishigami H., Horii H. (1993): Plane strain compression test of cemented sand and measurement of strain localization, Proc. Of 28th Anunal conference of Japan Geothenical Society, 545-548 (In Japanese).

9) Yashima, A., Matsumoto, A. and Tanabe, K. (2001): Slope failure at tunnel entrance due to excavation and its countermeasure, Modern Tunneling Science and Technology, Adachi et al (eds), IS-KYOTO2001, Vol. I, Balkema, 557-562.

10) Zhang, F., Yashima, A., Nakai, T., Ye, G.L. and Aung, H. (2005): An elasto-viscoplastic model for soft sedimentary rock based on tij concept and subloading yield surface. Soils and Foundations, 45(1), 65-73.

11) Zhang, F., Yashima, A., Ye, G. L., Aung, H., Naitou, K. and Nakai, T. (2006): Elasto-Viscoplastic Behavior of Soft Sedimentary Rock, Tests and Its Modeling. Geomechanics II, Proceedings of the Second Japan-U.S. Workshop on Testing, Modeling, and Simulation in Geomechanics, ASCE publications, 148-161.

APPENDIX

The Spatial Mobilized Plane (SMP) was defined by Nakai and Matsuoka (1986).

In tij clay and sand models, a symmetric tensor t_{ij} is expressed by a product of stress tensor σ_{ik} and a tensor a_{kj} as:

$$t_{ij} = \sigma_{ik} a_{kj} \tag{A-1}$$

where tensor a_{kj} can be evaluated by Cayley-Hamilton's theory as

$$a_{ij} = \sqrt{\frac{I_3}{I_2}} r_{ij}^{-1}, \quad r_{ik} r_{kj} = \sigma_{ij}, \quad r_{ij} = (\sigma_{ik} + \bar{I}_2 \delta_{ik})(\bar{I}_1 \sigma_{kj} + \bar{I}_3 \delta_{kj})^{-1} \tag{A-2}$$

where $\bar{I}_1$, $\bar{I}_2$ and $\bar{I}_3$ are the first, second and third invariants of stress tensor r_{ij} and I_2 and I_3 are the second and third invariants of stress tensor σ_{ij}.

A normal component t_N and a tangential component t_S of the principal-value vector of t_{ij} can be given as (see Figure A-1a),

$$\begin{aligned} & t_N = t_1 a_1 + t_2 a_2 + t_3 a_3 = t_{ij} a_{ij} \\ & \equiv \sigma_{SMP} = \sigma_1 a_1^2 + \sigma_2 a_2^2 + \sigma_3 a_3^2 = 3\frac{I_3}{I_2} \end{aligned} \tag{A-3}$$

$$\begin{aligned} & t_S = \sqrt{(t_1^2 + t_2^2 + t_3^2) - t_N^2} = \sqrt{t_{ij} t_{ij} - (t_{ij} a_{ij})^2} \\ & \equiv \tau_{SMP} = \sqrt{(\sigma_1 - \sigma_2)^2 a_1^2 a_2^2 + (\sigma_2 - \sigma_3)^2 a_2^2 a_3^2 + (\sigma_3 - \sigma_1)^2 a_3^2 a_1^2} \\ & = \frac{\sqrt{I_1 I_2 I_3 - 9 I_3^2}}{I_2} \end{aligned} \tag{A-4}$$

where I_1 is the first invariants of stress tensor σ_{ij}.

It is assumed that the directions of plastic principal strain increments coincide with those of principal axes of tij, and the plastic strain increment can also be given by a normal component ($d\varepsilon_{SMP}^{*P}$) and a tangential component ($d\gamma_{SMP}^{*p}$) of the principal plastic strain increment vector on the SMP (see Figure A-1b),

$$d\varepsilon_{SMP}^{*P} = d\varepsilon_1^P a_1 + d\varepsilon_2^P a_2 + d\varepsilon_3^P a_3 = d\varepsilon_{ij}^P a_{ij} \tag{A-5}$$

$$\begin{aligned} d\gamma_{SMP}^{*p} &= \sqrt{(d\varepsilon_1^{p2} + d\varepsilon_2^{p2} + d\varepsilon_3^{p2}) - d\varepsilon_{SMP}^{*p2}} \\ &= \sqrt{d\varepsilon_{ij}^p d\varepsilon_{ij}^p - (d\varepsilon_{ij}^p a_{ij})^2} \end{aligned} \tag{A-6}$$

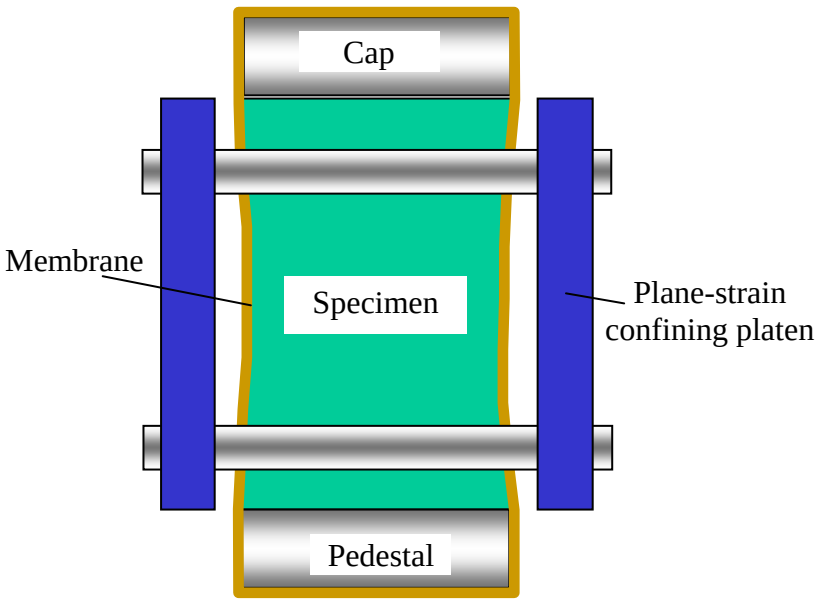

Fig. 1 Recessing deformation of soft geomaterial during isotropic consolidation

Fig. 2 Photo of plane-strain test apparatus

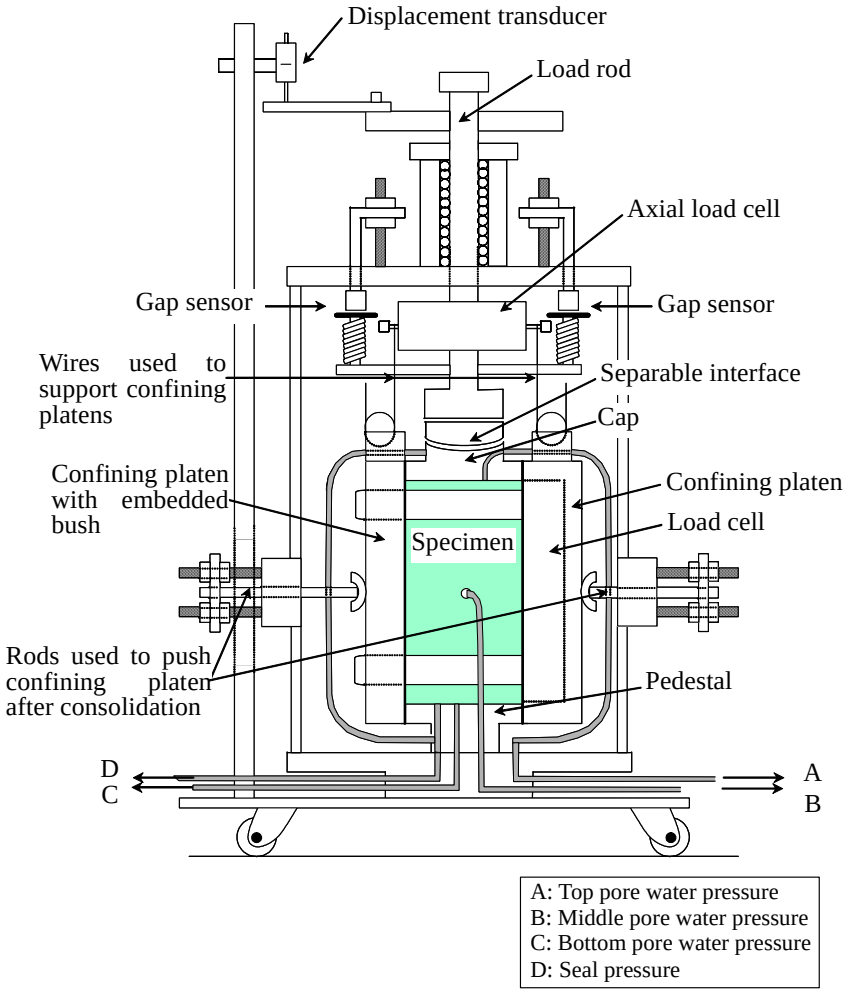

Fig. 3 Schematic illustration of hydraulic pressure cell

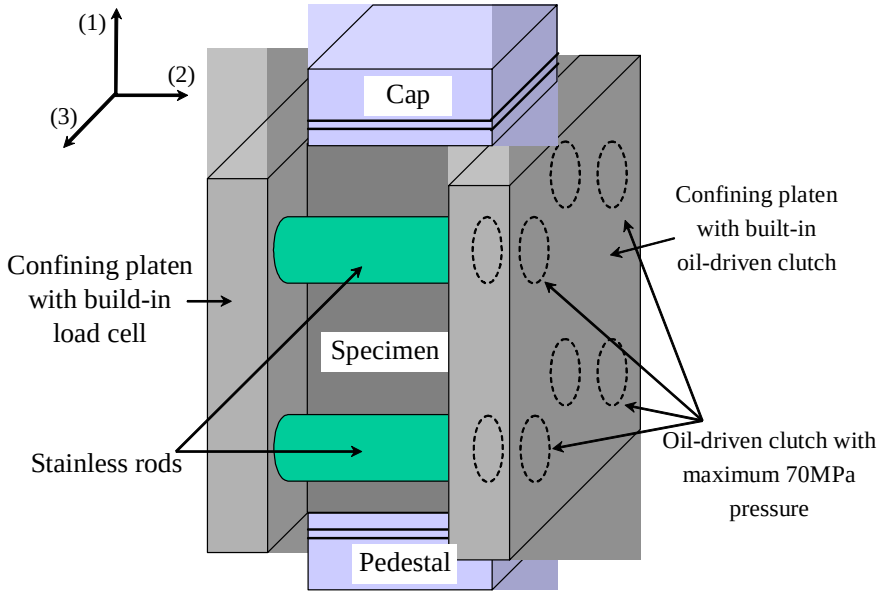

Fig. 4 Schematic illustration of plane-strain constraint device

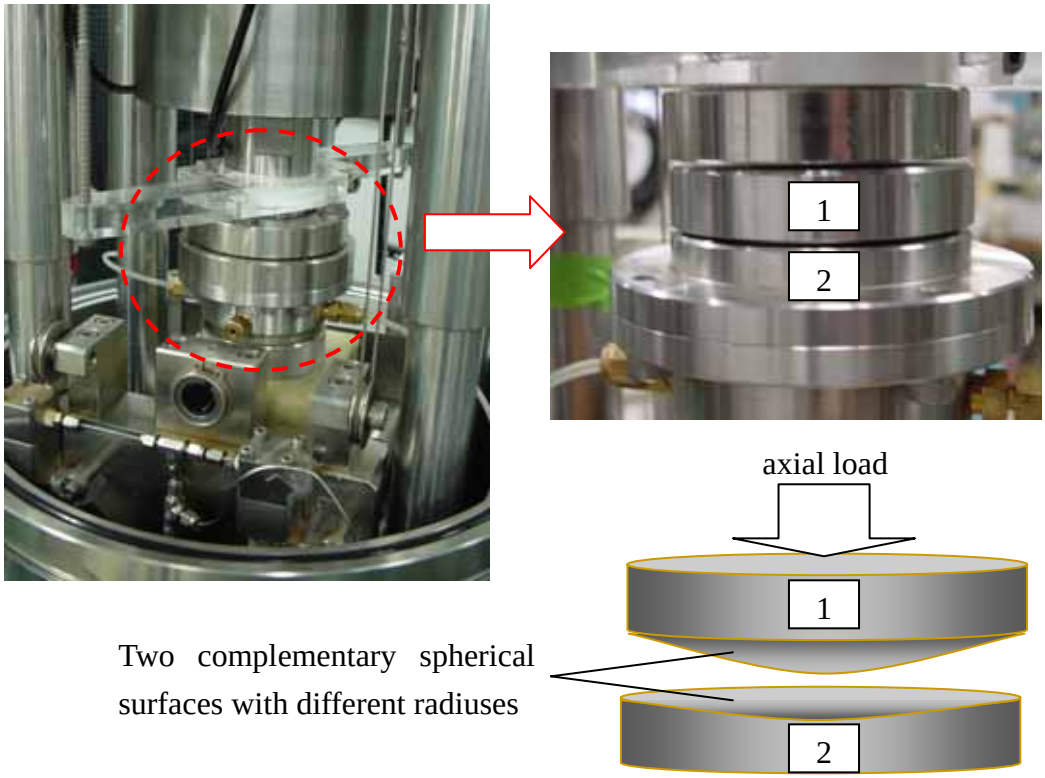

Fig.5 Photo of separable interface between axial load rod and cap

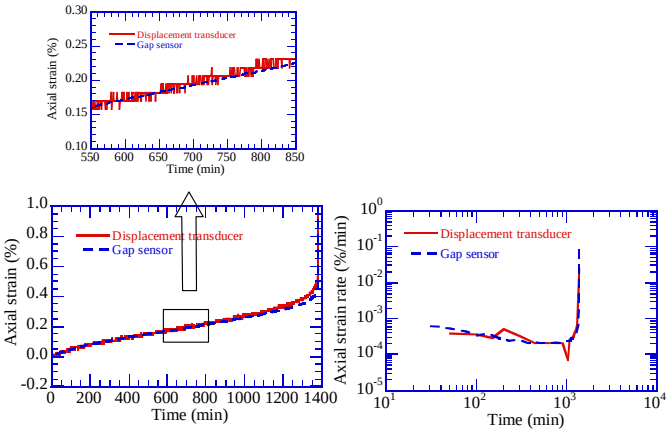

Fig. 6 Precision of displacement transducer (DT) and gap sensor

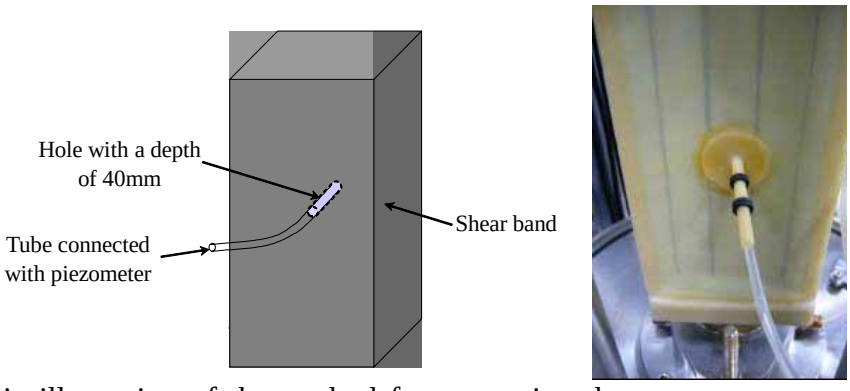

Fig. 7 Schematic illustration of the method for measuring the pore-water pressure in/near the shear band

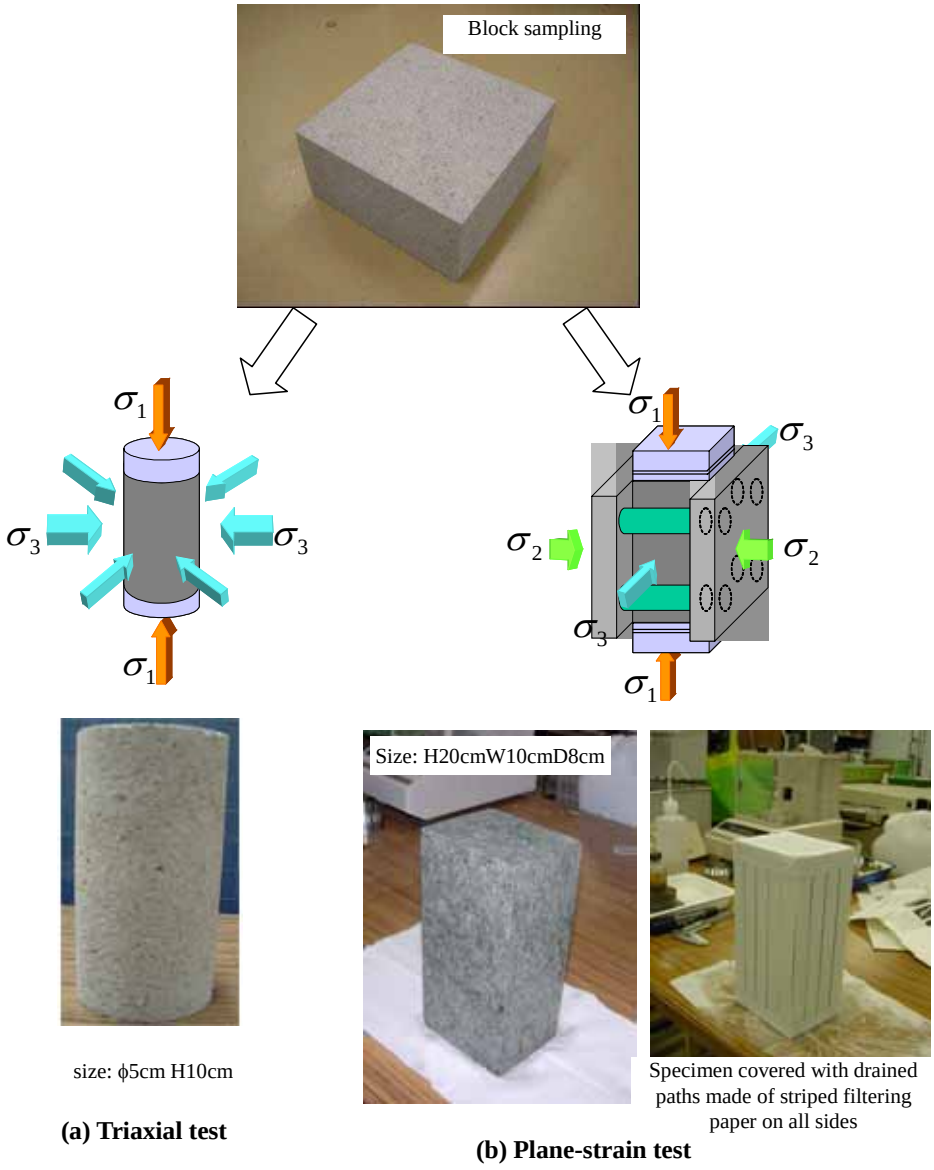

Fig.8 Specimen of soft sedimentary rock

(a) Evacuation in desiccate for certain time

(b) Replaced with carbon dioxide gas

(c) Replaced with gas-free water and evacuated again for certain time

Fig.9 Saturation of specimen (B value >0.95)

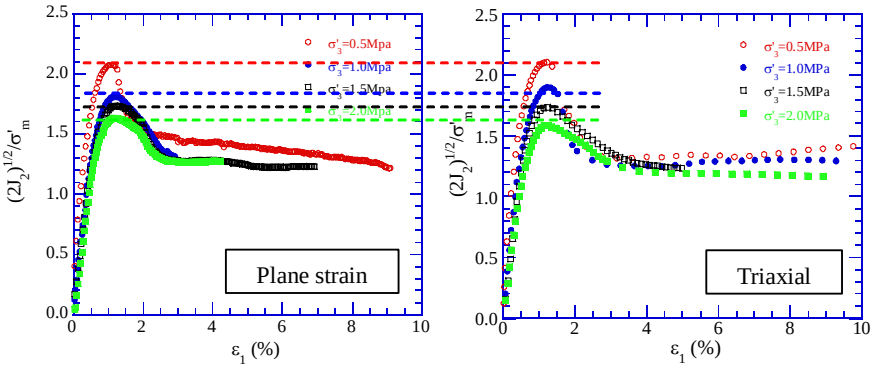

(a) Stress ratio $\sqrt{2J_2}/\sigma_m^{'}$

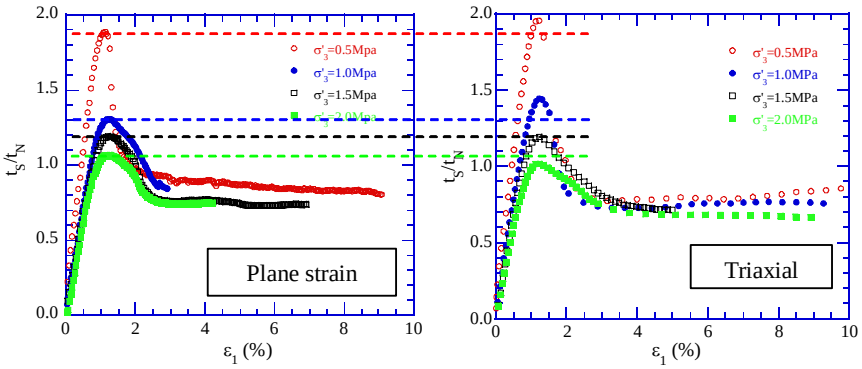

(b) Stress ratio t_S/t_N

Fig. 10 Comparison of peak values of different types of stress ratios under plane-strain compression and triaxial compression

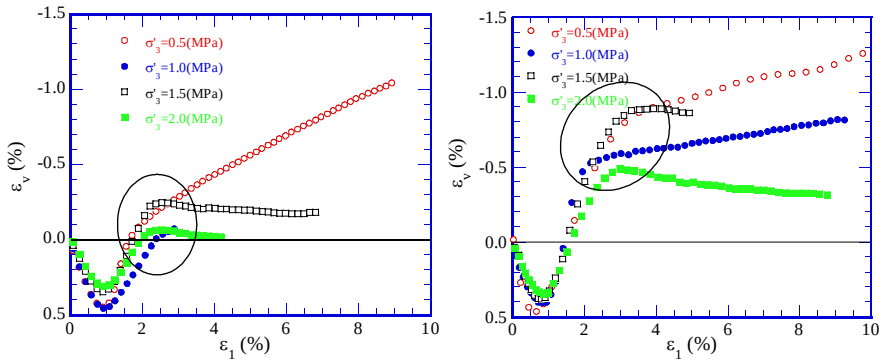

(a) Plane-strain compression (b) Triaxial compression

Fig. 11 Comparison of volumetric strain under plane-strain compression and triaxial compression

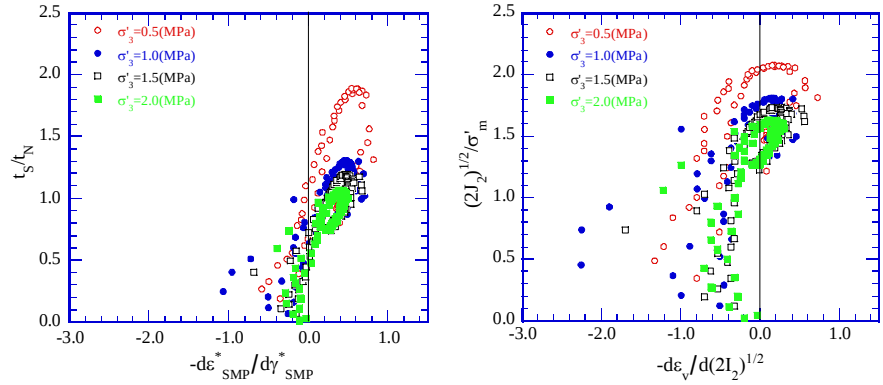

(a) Plane-strain compression

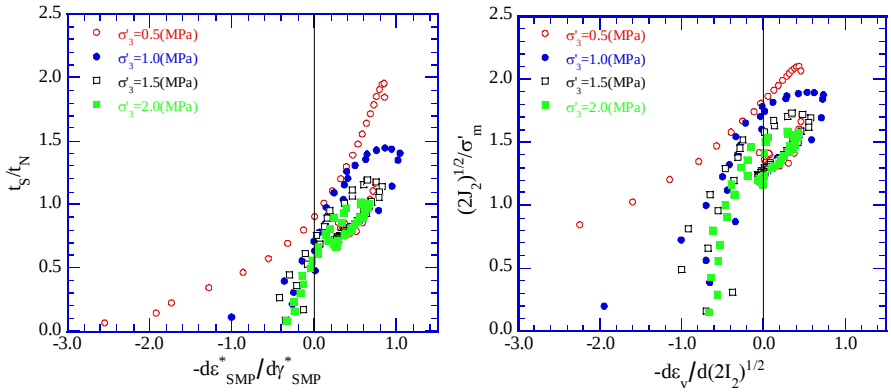

(b) Triaxial compression

Fig. 12 Stress-dilatancy relations in different stress spaces

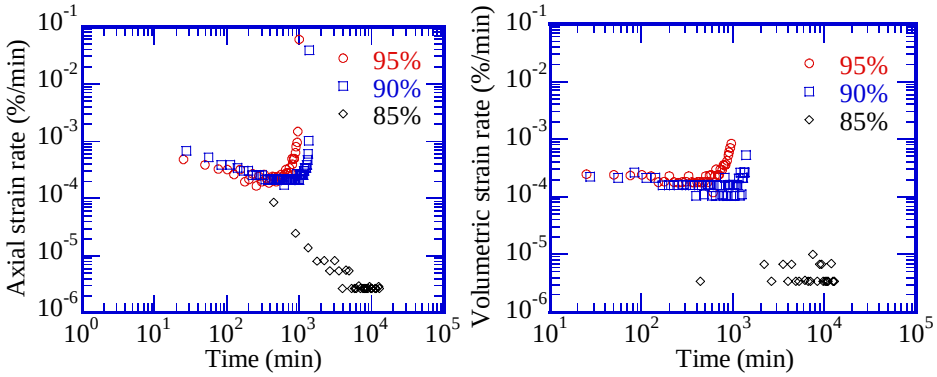

Fig. 13 Strain rate vs. time in plane-strain creep test

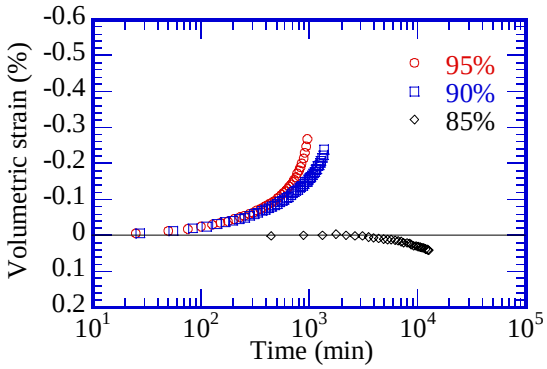

Fig. 14 Volumetric strain vs. time in plane-strain creep test

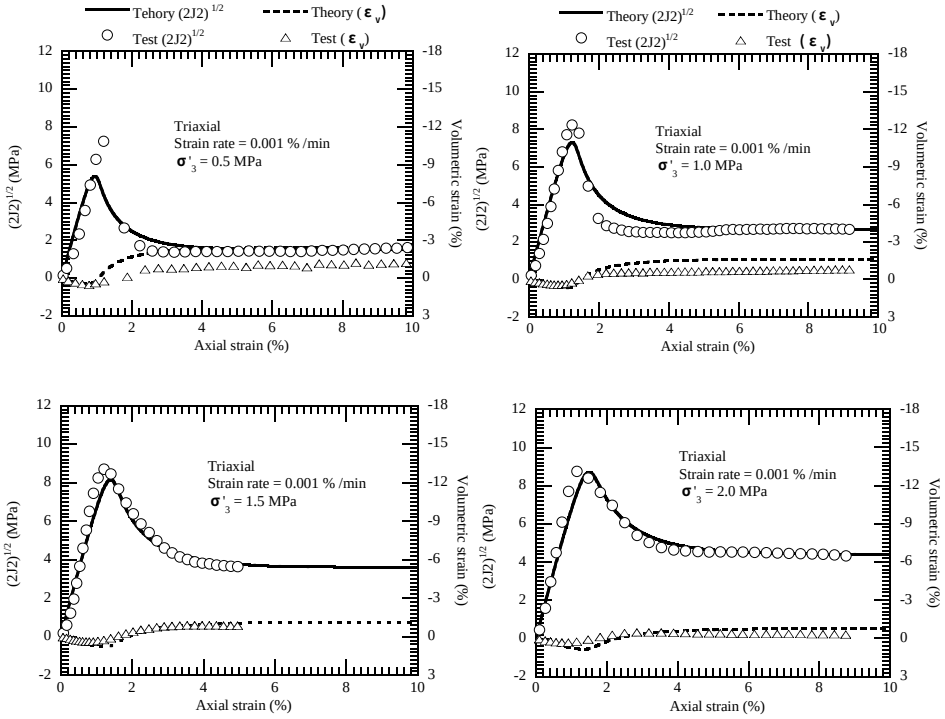

Fig.15 Verification of the predicted stress-strain-dilatancy relations under triaxial loading (tests by Takigawa, 2003)

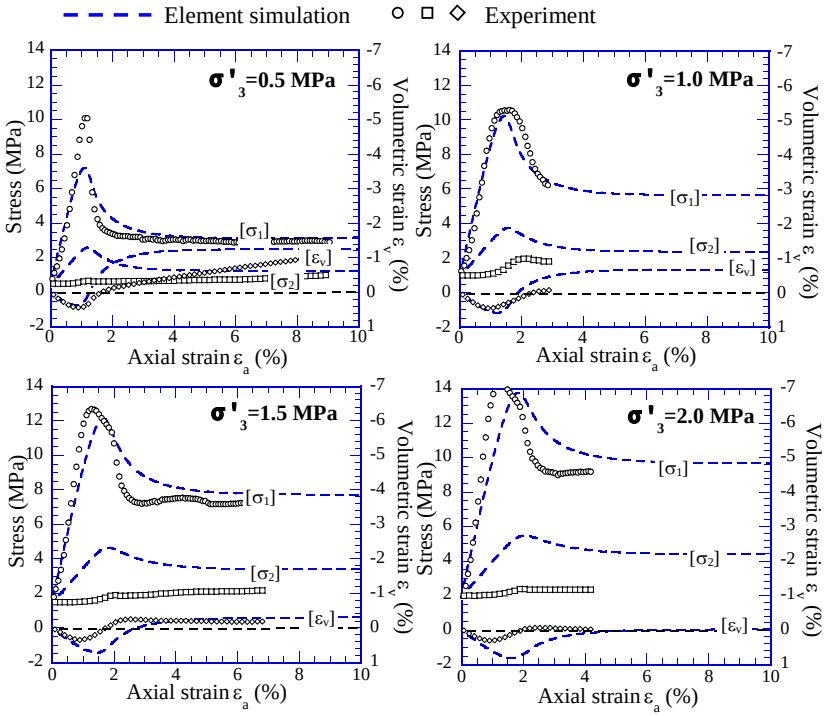

Fig. 16 Element simulation of constant strain-rate controlled drained plane-strain compression tests

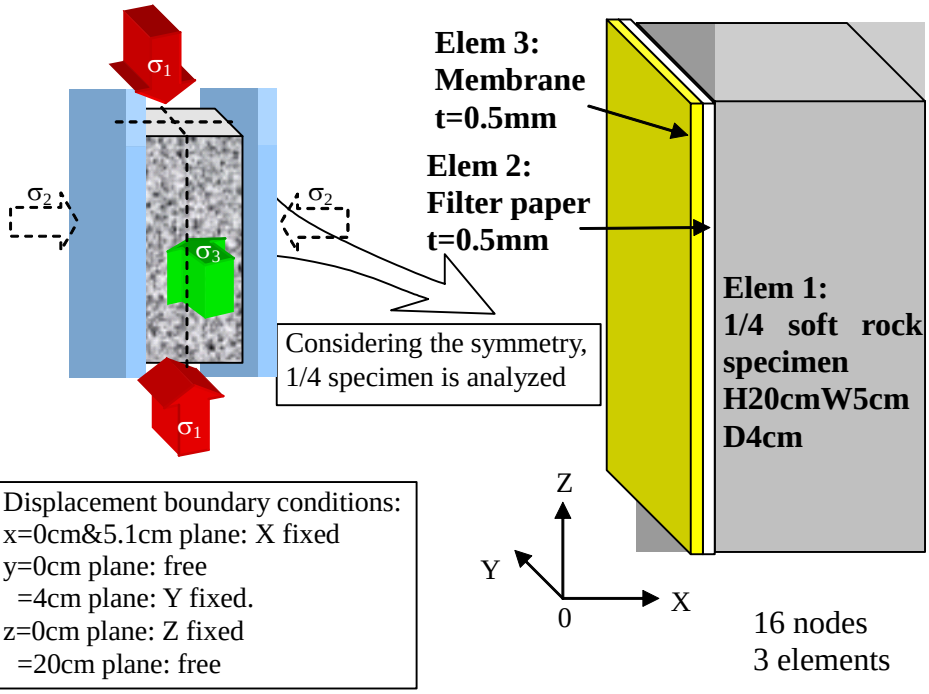

Fig.17 FEM model for analyzing the influence of boundary conditions to σ_2

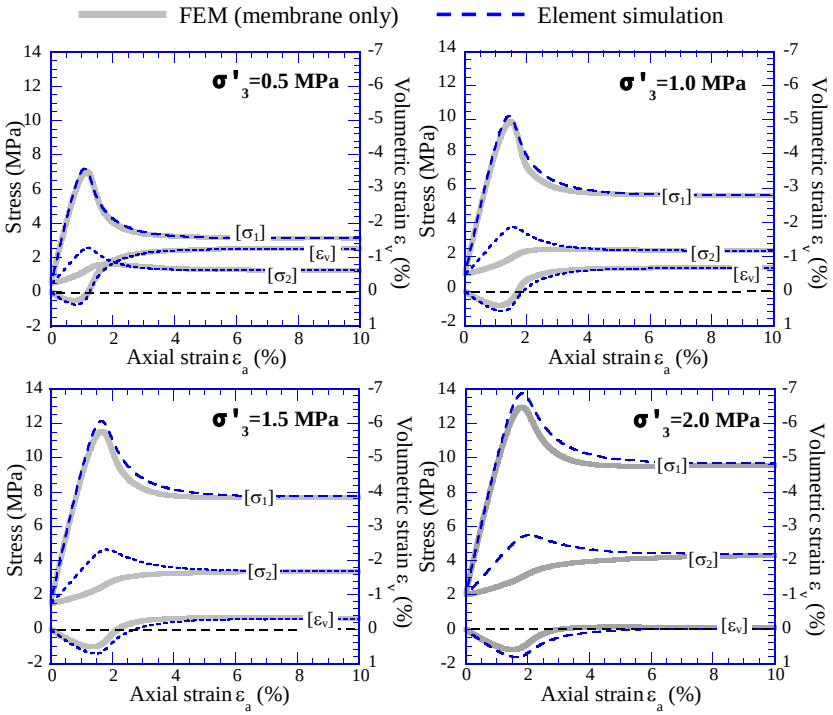

Fig. 18 Comparison of FEM (membrane only) and element simulation results of Ohya Stone

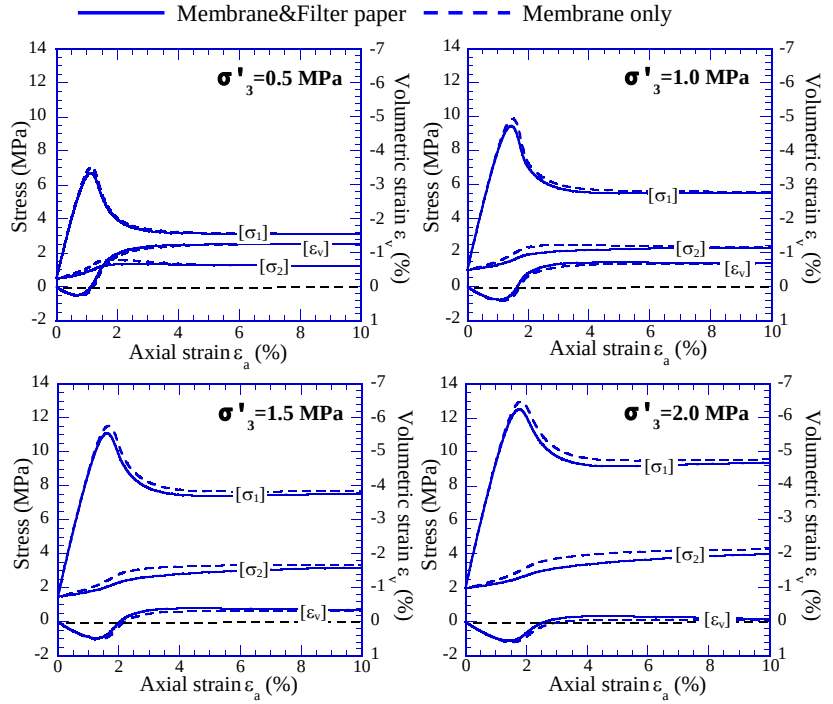

Fig. 19 FEM calculation considering the influence of both membrane and filter paper

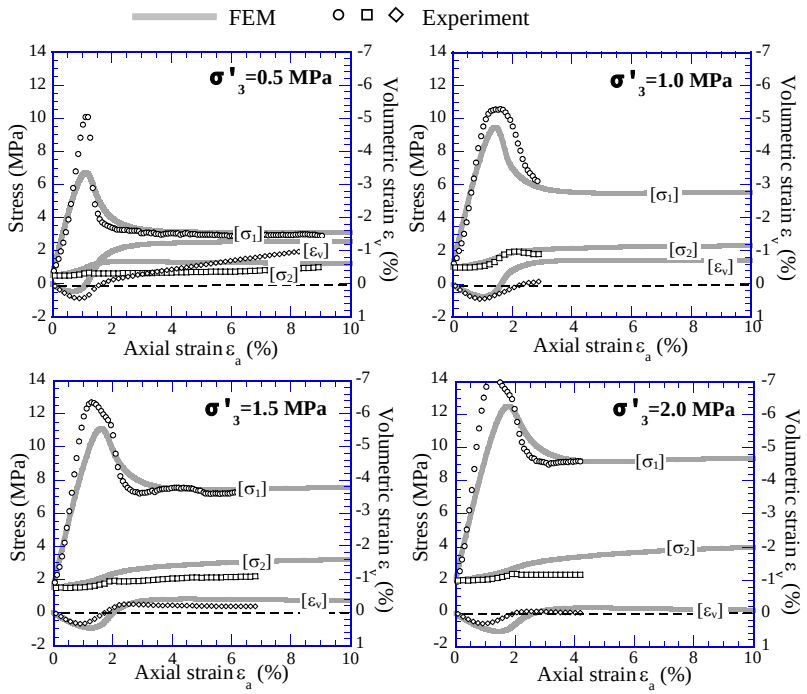

Fig. 20 Comparison of FEM and experiment results of Ohya Stone

Fig. 21 Photos of rubber block specimen with/without membrane

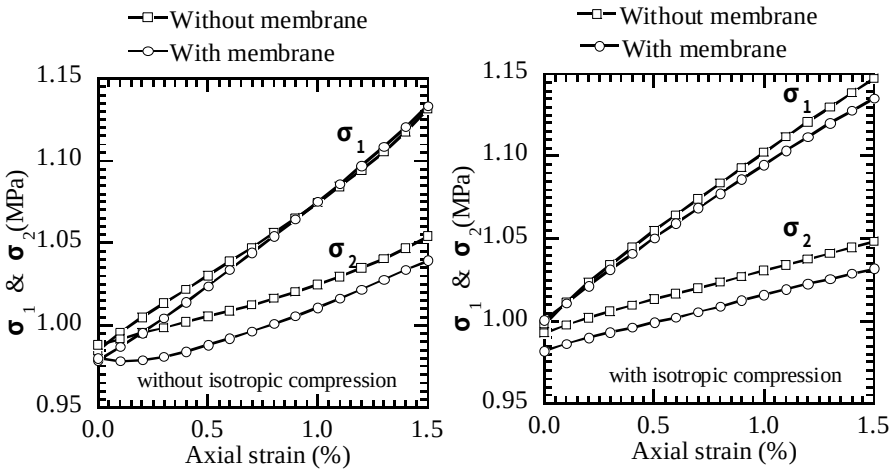

Fig. 22 Stress-strain relation on rubber specimen in plane-strain compression test

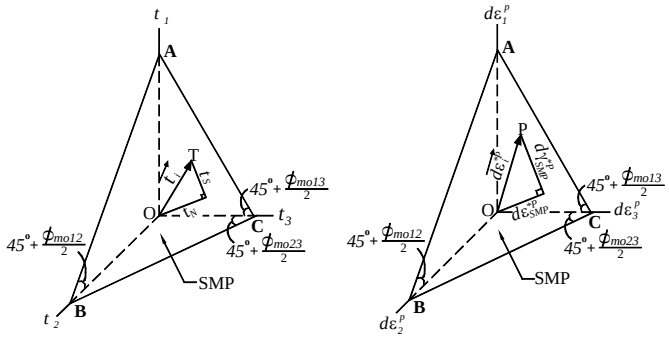

(a) t_s and t_n expressed in principal stress space of t_{ij} tensor

(b) Increment strain expressed in principal increment strain space of $d\varepsilon_{ij}$ tensor

Fig. A-1 Explanation of stress and strain in principal-value space of tensor t_{ij}(Nakai, 1989)

Table 1 Drained compression tests under constant strain rate

	Case1	Case2	Case3	Case4
$\dot{\varepsilon}_1$ (%/min)	0.001	0.001	0.001	0.001
σ'_3 (MPa)	0.5	1.0	1.5	2.0

Table 2 Drained creep tests

	Case5	Case6	Case7
Axial load rate (kN/min)	0.05	0.05	0.05
Creep stress (MPa)	7.45 (95%*)	7.10 (90%*)	6.67 (85%*)
Confining stress σ'_3 (MPa)	1.0	1.0	1.0

*Creep stress is the percent of peak strength obtained from the constant-strain-rate drained compression test under the same confining stress.

Table 3 Physical properties of Ohya Stone

Initial void ratio e_i	0.44
Specific gravity of soil particles G_s	2.51
Initial consolidation yielding stress p'_c (MPa)	30.0

Table 4 Material parameters involved in the model for Ohya Stone

Confining pressure σ'_{30} (MPa)	0.5	1.0	1.5	2.0
Young modulus E (MPa)	900.0			
Poisson's ratio ν	0.25			
Stress ratio at critical state R_f	4.60	4.20	3.90	3.70
Plastic modulus E_p ($=\lambda$-κ)	0.0125			
Stress-dilatancy parameter β	1.5			
Time-dependency parameter α	0.75			
Time-dependency parameter C_n	0.02			
Evolution parameter of OCR a	850			
Axial strain rate (%/min)	0.001			
Standard void ratio at p'=98kPa	0.95			

Table 5 Material parameters for membrane and filter paper

	Membrane	Filter paper
Young modulus E (MPa)	1.0	1.0
Poisson's ratio ν	0.4	0.4